JACS Au
AN OPEN ACCESS JOURNAL OF THE AMERICAN CHEMICAL SOCIETY

pubs.acs.org/jacsau

Letter

Defective PtRuTe As Nanozyme with Selectively Enhanced Peroxidase-like Activity

Changshuai Shang, Qingqing Wang, Hao Tan, Shiyu Lu, Shuguang Wang, Qinghua Zhang, Lin Gu, Jing Li,* Erkang Wang, and Shaojun Guo*

Cite This: *JACS Au* 2022, 2, 2453−2459

Read Online

ACCESS | Metrics & More | Article Recommendations | Supporting Information

ABSTRACT: Noble metal based nanozymes show great potential in replacing natural enzymes; however, their development is greatly restricted by their relatively low specificity and activity. Herein, we report the synthesis of a class of amorphous/crystalline PtRuTe nanomaterials with a Pt/Te-enriched core and a Ru-enriched shell as efficient peroxidase mimics with selectively enhanced peroxidase-like activity and suppressed oxidase-like activity. We demonstrate that amorphous domains play a critical role in tuning and optimizing the catalytic properties. The PtRuTe nanozyme with high-percentage defects exhibits superior catalytic activities and kinetics, and the suppressed oxidase-like activity could diminish the interference of O_2 in the glucose colorimetric assay. The high catalytic performance can be caused by amorphous phase induced electron redistribution and electronic interactions between different elements and the synergistic effect of multimetallic nanocrystals. The concurrent extraordinary peroxidase-like activity and suppressed oxidase-like activity guarantee the amorphous/crystalline PtRuTe nanozymes as promising alternatives of natural enzymes for biosensing and beyond.

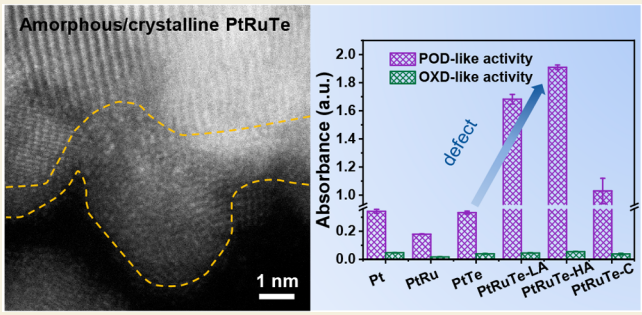

KEYWORDS: *defect, amorphous, noble metal, peroxidase nanozyme, specificity*

INTRODUCTION

Nanozymes can mimic the activities and functionalities of natural enzymes and show great potential for replacing them in the fields of biosensing, therapeutics, and imaging.[1−4] Compared with natural enzymes, nanozymes have obvious advantages in high tolerance to harsh conditions, low cost, tunable catalytic performance, and ease of mass production.[1] Nowadays, various nanomaterials including noble metals, metal oxides, and metal−organic frameworks (MOFs) as well as carbon-based nanomaterials, have been reported to possess intrinsic enzyme-like characteristics.[5−8] However, although great efforts have been devoted to nanozymes, their catalytic activities usually cannot match the kinetics of natural enzymes, which hinders their further application.[9] Moreover, due to the great complexity of nanomaterials, nanozymes invariably show unsatisfactory specificity with multiple enzyme-mimicking performances.[10] This is also undesirable, especially for peroxidase nanozymes in colorimetric assay.[11] Therefore, constructing nanozymes with high specificity and satisfactory activity is of great significance in broadening their application and disclosing the underlying property enhancement mechanisms.[12]

Among the vast varieties of nanozymes, noble metal-based nanocrystals have drawn particular interest mainly due to their relatively higher catalytic efficiencies.[13] In addition, the inert feature of noble metals endows them with outstanding resistance to extremely corrosive conditions. Therefore, noble metal nanozymes usually exhibit intriguing storage stabilities.[14] The catalytic performances of noble metal nanocatalysts can be further promoted by regulating the electronic states and taking advantage of the synergistic effect.[15] In this regard, the commonly used strategies include elemental composition tailoring and defect engineering, of which amorphization of nanomaterials has drawn increasing attention because of the favorable structures and properties of derived defects.[16−19] Different from close-packed crystalline noble metal materials with periodic atomic arrangement, amorphous nanomaterials are composed of randomly distributed atoms, and only exhibit local short-range order.[20] The inherent disordered feature means randomly oriented bonds, which can cause electron redistribution and potentially provide enormous catalytically active defects and unsaturated atoms on the surface.[17,18,21,22] In addition, benefiting from isotropic properties without

Received: September 12, 2022
Revised: October 11, 2022
Accepted: October 12, 2022
Published: October 30, 2022

https://doi.org/10.1021/jacsau.2c00495
JACS Au 2022, 2, 2453−2459

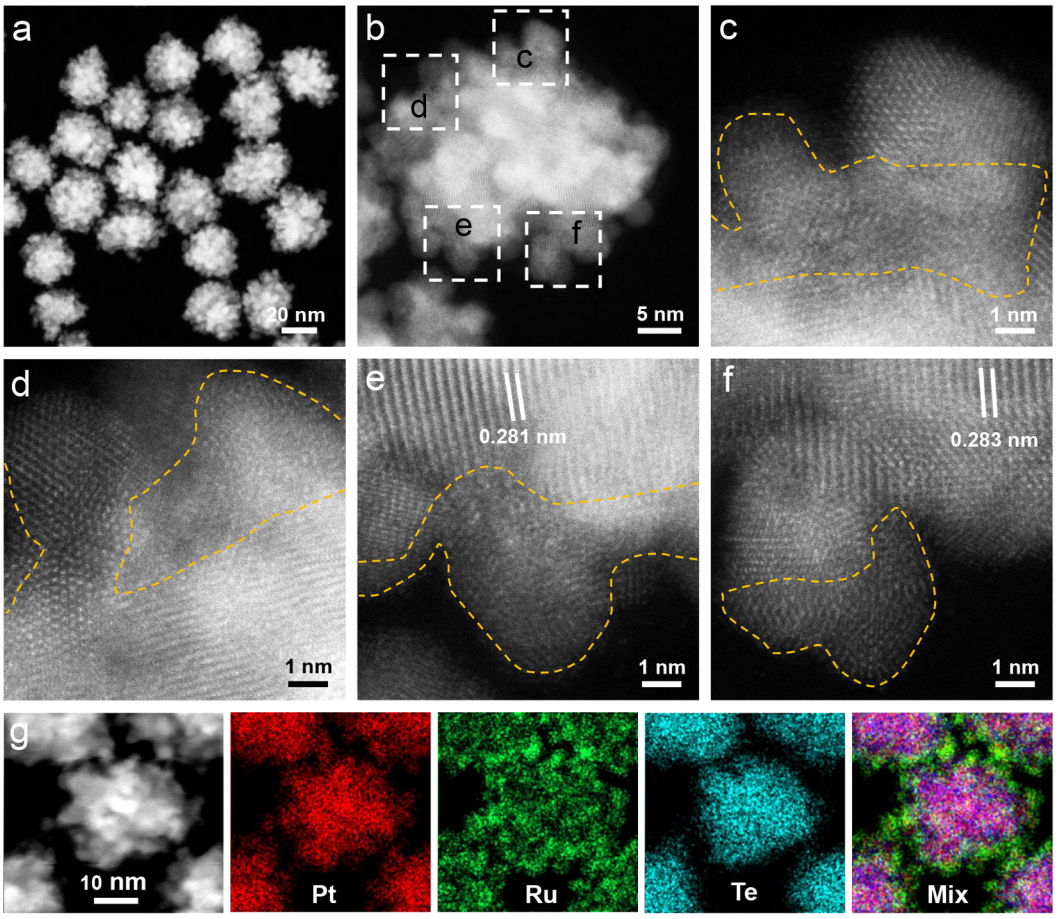

Figure 1. Typical (a) TEM and (b) HAADF-STEM images of PtRuTe-HA nanomaterials. (c–f) Corresponding HAADF-STEM images of areas marked with white squares in panel b. Amorphous structures are marked with orange dashed lines. (g) HAADF-STEM and elemental mapping of individual PtRuTe-HA nanomaterial.

physicochemical heterogeneities, amorphous materials exhibit ultrahigh corrosion resistance and pave the way for searching highly stable catalysts.[23−25]

Herein, we develop a new method for making the amorphous/crystalline PtRuTe nanomaterials with abundant amorphous domains as highly efficient peroxidase mimics. The highly amorphous PtRuTe nanozymes, consisting of a Pt/Te-enriched core and a Ru-enriched shell, show much higher enzyme-like activities than their crystalline PtTe, PtRu, and Pt counterparts, with their initial reaction rate being 10.5 times that of Pt nanoparticles. Most importantly, highly amorphous PtRuTe nanomaterials show intriguing enzymatic specificity with greatly suppressed oxidase-like activities. With H_2O_2 as intermediary, a simple detection platform for glucose is achieved with a wide linear range from 3 to 500 μM and a low detection limit of 1.52 μM, demonstrating that these nanomaterials have great potential as a substitute for natural horseradish peroxidase (HRP) in biosensing.

RESULTS AND DISCUSSION

Amorphous/crystalline PtRuTe nanomaterials with high-density amorphous phases (denoted as PtRuTe-HA) were prepared by a simple solvothermal method, in which $Pt(acac)_2$, $Ru(acac)_3$, and $Te(OH)_6$ were coreduced by phloroglucinol in the presence of $Mo(CO)_6$. Transmission electron microscopy (TEM) results (Figure 1a and Figure S1) indicate that the products possess walnut kernel-like morphology in high purity, and their mean size is about 33.0 ± 4.1 nm. High-angle annular dark-field scanning transmission electron microscopy (HAADF-STEM) images of PtRuTe-HA (Figure 1b and Figure S2a) prove their highly irregular surface is enclosed with dense tiny bulges. Atomic-resolution HAADF-STEM images (Figure 1c–f and Figure S2b–e) reveal that most atoms on the near surface are randomly distributed without forming regular and complete lattice fringes, a typical characteristic of amorphous structures.[20] In the meantime, the interior regions show clear periodic lattice fringes. Specifically, the lattice fringe spacings of 0.281 and 0.283 nm are close to the interplanar distance of the $PtTe_2$ (101) plane.[26] The elemental mapping and line scanning of PtRuTe (Figure 1g and Figure S2f) verify that Pt, Ru, and Te atoms are distributed throughout the whole PtRuTe-HA, while the core is Pt and Te enriched, and the shell is Ru enriched (with darker color). The atomic ratio of Pt:Ru:Te in PtRuTe-HA is determined to be around 22:35:43 by scanning electron microscopy energy-dispersive X-ray spectroscopy (SEM-EDS) result (Figure S4). To clearly understand the formation process of PtRuTe-HA, we monitored the structural and compositional variations of the intermediate products at different reaction stages. As shown in TEM images (Figure S3), the initially formed product (t = 40 min) has a smooth surface with a relatively smaller size. The Ru content was measured to be about 5%, which was gradually increased with the prolonged reaction times, suggesting that Pt and Te precursors were preferentially reduced under current

https://doi.org/10.1021/jacsau.2c00495
JACS Au 2022, 2, 2453−2459

reaction conditions.[27] In addition, the surfaces and sizes of products became severely irregular and slightly larger with increasing reaction time. These phenomena indicate that the introduction of Ru into PtTe nanomaterials can contribute to the formation of amorphous structure.

It is worth noting that PtRuTe nanomaterials with similar profiles but different elemental contents can be facilely synthesized by varying the adding amounts of $Ru(acac)_3$. As shown in Figure 2a, b, when fewer Ru precursor was introduced, the resulting PtRuTe nanomaterials exhibited more complete sheetlike morphology with fewer tiny tips located on the surface. These structural differences indicate that the density of amorphous domains on the current nanomaterial might be lower than highly amorphous PtRuTe-HA (denoted as PtRuTe-LA). Moreover, in the absence of $Ru(acac)_3$, the synthetic protocol led to the formation of sheet-like PtTe nanomaterials (Figure 2c) with perfectly smooth surfaces. The average sizes of PtTe and PtRuTe-LA were estimated to be 52.1 ± 6.2 and 44.7 ± 5.5 nm, while the atomic ratios of Pt:Te and Pt:Ru:Te were 34:66 and 28:23:49 (Figures S4–S6), respectively. More crystalline properties were disclosed by powder X-ray diffraction (PXRD) measurements. As shown in Figure 2d, all the diffraction peaks of the as-synthesized three kinds of nanomaterials matched well with the standard diffraction patterns of $PtTe_2$ (18–0977). The diffraction peaks of PtRuTe-LA and PtRuTe-HA come from the internal crystalline regions since amorphous phases cannot produce diffraction peaks.[28] This phenomenon is also evidence that Ru atoms of internal crystalline domains might exist in the substitution form.[29]

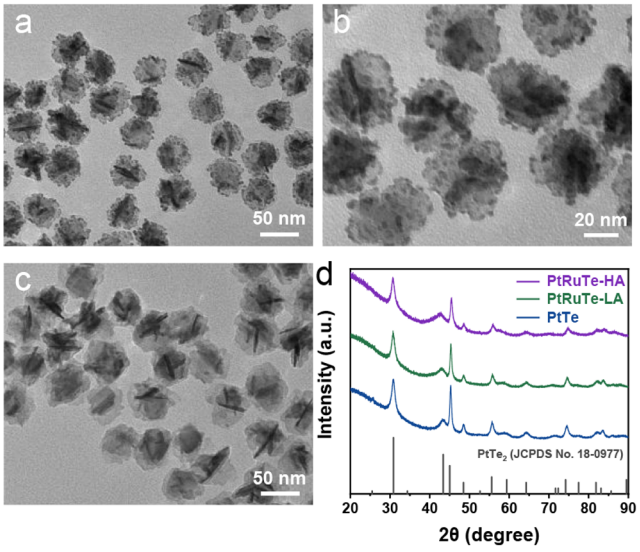

Figure 2. Representative TEM images of (a, b)PtRuTe-LA and (c) PtTe. (d) PXRD patterns of various nanomaterials.

Inspired by the intriguing amorphous domain of PtRuTe-HA nanomaterials, we investigated their peroxidase-like activities and compared them with those of PtRuTe-LA, PtTe, and commercially available Pt and PtRu nanoparticles. Moreover, the PtRuTe nanomaterial (PtRuTe-C) with the same composition as PtRuTe-HA but better crystallinity (Figures S7 and S8) was prepared by annealing PtRuTe-HA at 250 °C for 5 h in Ar and 250 °C for 1 h in air. The oxidation of TMB (3,3′,5,5′-tetramethylbenzidine) by H_2O_2 was adopted as a model colorimetric reaction. As shown in Figure 3a, the much higher peak intensity at 450 nm, belonging to the two-electron oxidation product of TMB, is observed, meaning that

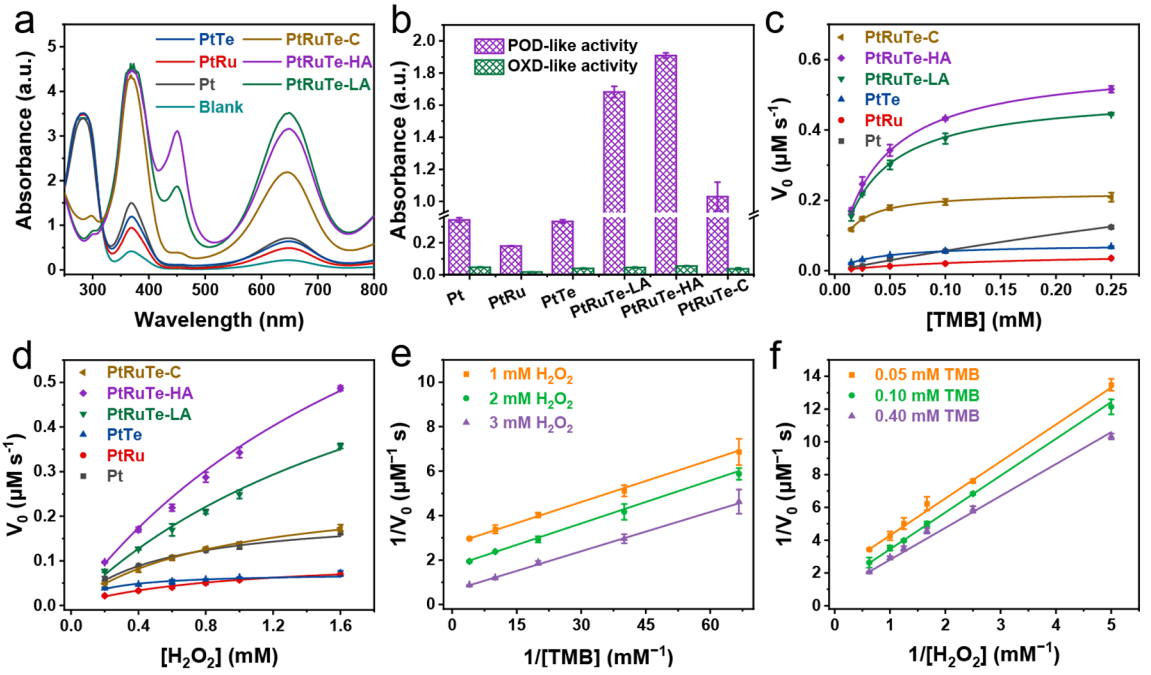

Figure 3. (a) UV–vis spectra of the reaction solutions catalyzed by different nanozymes with the same nanozyme dosages at t = 1 min. (b) Peroxidase (POD) and oxidase (OXD)-like activities of different nanozymes at t = 30 s. Typical Michaelis–Menten curves of various nanozymes by changing the concentrations of (c)TMB and (d) H_2O_2. Double reciprocal plots against TMB at (e) three fixed H_2O_2 concentrations or (f) against H_2O_2 at three fixed TMB concentrations in the presence of PtRuTe-HA.

https://doi.org/10.1021/jacsau.2c00495
JACS Au 2022, 2, 2453–2459

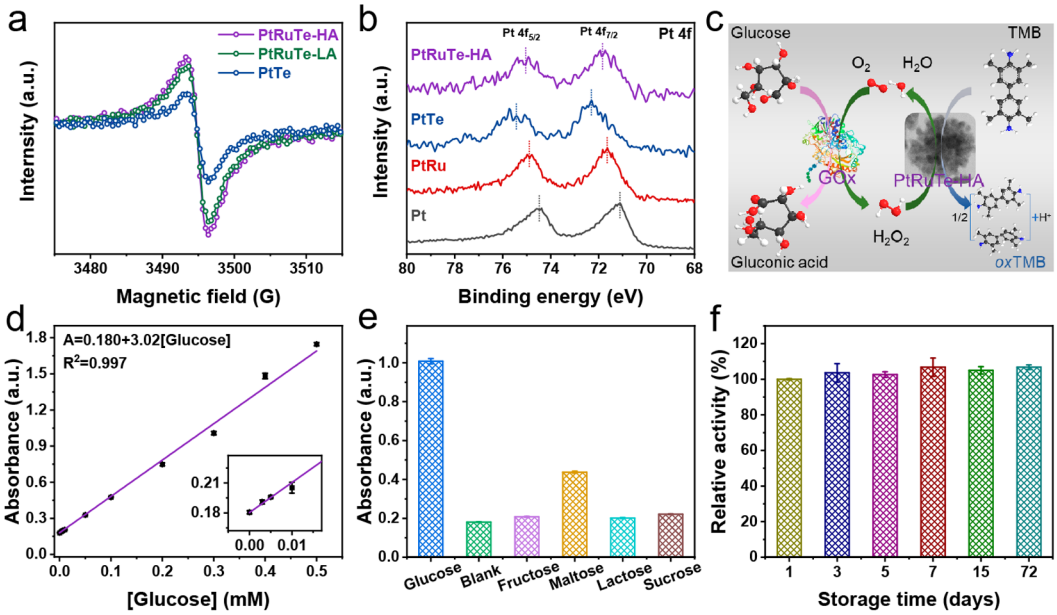

Figure 4. (a) ESR and (b) Pt 4f XPS spectra of various nanomaterials. (c) Schematic illustration, (d) calibration curve, and (e) selectivity test of glucose detection. (f) Storage stability of the PtRuTe-HA nanozyme.

PtRuTe-HA can efficiently accelerate the colorimetric reaction, demonstrating their superior catalytic activity.[30] It is worth noting that PtRuTe-HA also exhibits much better catalytic specificity with greatly enhanced peroxidase-like activity and nearly similar oxidase-like activity (Figure 3b). The improved specificity can contribute to their wider application by diminishing the reaction between substrates and O_2.[11,15]

To gain more insights into the catalytic kinetics, the apparent steady-state kinetics were tested, and Michaelis–Menten curves were obtained by plotting the initial reaction velocities against concentrations of TMB or H_2O_2. The apparently higher initial reaction velocities of PtRuTe-HA (Figure 3c, d) than other counterparts further verified their enhanced catalytic activities. The catalytic activities follow the sequence of PtRuTe-HA > PtRuTe-LA > PtTe, coinciding with the densities of the amorphous structure. Specifically, the initial reaction velocity (Figure S9) of PtRuTe-HA at 0.05 mM TMB and 2 mM H_2O_2 is 0.342 μM s^{-1}, which is 10.5, 26.3, and 8 times higher than those of Pt, PtRu, and PtTe, respectively.

The Michaelis constants (K_m) of various catalysts were calculated based on the double-reciprocal plots (Figures S10 and S11), derived from the Michaelis–Menten curves. For as-prepared PtRuTe-HA, PtRuTe-LA, PtRuTe-C, and PtTe nanozymes, their K_m values (Table S1) against TMB are similar to each other but are all much lower than Pt, PtRu, as well as many reported noble metal nanozymes and single-atom Fe–N–C nanozymes.[13,31] These results suggest that PtRuTe-HA possesses an ultrahigh affinity toward TMB, and the introduction of Te may be conducive to improving affinity. The K_m value of PtRuTe-HA when using H_2O_2 as substrate is higher than others, meaning that more H_2O_2 is needed to reach the maximal reaction activity for PtRuTe-HA.[32] In addition, we measured and compared the catalytic activities of PtRuTe-HA among a range of substrate concentrations with three fixed concentrations of another substrate. The nearly parallel plots (Figure 3e, f) reveal that the catalytic process follows the ping-pong mechanism, similar to HRP and ferromagnetic nanoparticles.[7] This means that PtRuTe-HA nanozyme reacts with the first substrate and releases the first product before the subsequent reactions with the second substrate. Like the catalytic properties of HRP, peroxidase-like activities of PtRuTe-HA also depend on the pH and temperature (Figure S12) of the reaction solutions.

The novel highly amorphous structures together with suitable components of PtRuTe-HA are believed to be responsible for substantially promoted catalytic activities and specificities.[33] To quantitatively compare the amorphous phase density and prove the positive effects of density on catalytic activity, we conducted electron spin resonance (ESR) measurements to verify the defect-related unpaired electrons.[31] The peak intensity (Figure 4a) follows the order of PtRuTe-HA > PtRuTe-LA > PtTe, demonstrating the enriched density of the amorphous phase in PtRuTe-HA, consistent with the direct TEM observation. In addition, PtRuTe-C exhibits inferior peroxidase-like activity (Figure 3b) compared to PtRuTe-LA and PtRuTe-HA. These results clearly prove the essential role of amorphous defects in improving the peroxidase-like activity. The oxidase-like activity (Figure 3b) of PtRuTe-C is also quite low and similar to others, which means that apart from amorphous defects, the suppressed oxidase-like activity may also be influenced by the suitable component. X-ray photoelectron spectroscopy (XPS) technique was further adopted to disclose the electronic state variations of different nanomaterials. As shown in Figure 4b, two main peaks that belong to Pt $4f_{7/2}$ and Pt $4f_{5/2}$ can be found.[34] Moreover, compared with commercial Pt nanoparticles, the binding energies of Pt 4f for PtTe and commercial PtRu nanoparticles obviously shifted to higher values, indicating the electron transferred from Pt to Te or Ru.[27] As for PtRuTe-HA, the Pt 4f binding energy was slightly higher than that of PtRu, probably caused by the electron transfer between different elements and amorphous phase induced electron redistribution.[18,35] Previous works imply that the peroxidase-like specificity is affected by the adsorption abilities of H_2O_2 and O_2 while the catalytic efficiency is tailored

https://doi.org/10.1021/jacsau.2c00495
JACS Au 2022, 2, 2453–2459

by oxidation of TMB and desorption of HO*/O*.[14,15] The regulated electronic states of PtRuTe-HA can undoubtedly influence the adsorption behavior of substrates and various reaction intermediates and modulate the catalytic performances by changing the Gibbs free energies of H_2O_2 decomposition and the O_2 dissociation reaction.[14,36−39] Apart from electronic interactions, the synergistic effects of multimetallic nanozymes also contribute to improved catalytic performances.[37] Collectively, the enriched catalytically active defects in amorphous phases and the electronic and synergistic effects of multimetallic nanomaterial enable the promising peroxidase-like properties of PtRuTe-HA.

Given the outstanding peroxidase-like activity and suppressed oxidase-like activity of PtRuTe-HA, a cascade catalytic process was established for the colorimetric detection of glucose (Figure 4c).[40,41] As exhibited in Figure 4d, the absorbances of oxidized TMB at 652 nm increase with the elevated glucose concentrations, and show a good linear relationship (R^2 = 0.997) within the concentration ranges from 3 μM to 500 μM and a low detection limit of 1.52 μM (S/N = 3), superior to many reported nanomaterials (Table S2). The selectivity of this detection method was investigated by measuring and comparing the signals of many other similar substances. Although the concentrations of control samples were ten times that of glucose, their response signals were still much lower (Figure 4e) and can even be distinguished with naked eye based on the color difference (Figure S14). The splendid selectivity of this method was ascribable to the good specificity of glucose oxidase and PtRuTe-HA.[42] One-hundred-fold diluted fetal bovine serum was taken as a real sample. The good feasibility of the PtRuTe-HA-based biosensor for practical application was proved with spike recoveries (Table S3) ranging from 94.0 to 94.5% with a relative standard deviation (RSD) lower than 2.4%, comparable to that reported in the literature.[41] The excellent stability of the PtRuTe-HA nanozyme should also be emphasized, evidenced by the nearly unchanged catalytic activity after being stored at room temperature for more than 70 days (Figure 4f).

CONCLUSIONS

In summary, we achieved successful synthesis of amorphous/crystalline PtRuTe-HA nanozymes featuring abundant amorphous structures. The obtained nanozymes exhibit greatly enhanced peroxidase-like activity, with more than 10 times higher initial reaction velocities than Pt nanoparticles, and selectively suppressed oxidase-like activity. The synergistic effect of different elements in PtRuTe-HA and modulated electronic states that derived from novel amorphous phases and strong electronic interactions between Pt and Ru/Te are responsible for their remarkable catalytic performance. The excellent peroxidase-like specificity endows the PtRuTe-HA nanozyme with highly diminished disturbance of O_2. Consequently, the highly amorphous PtRuTe-HA nanozyme-based biosensor shows a wide linear range and a low detection limit of 1.52 μM for glucose detection as well as prominent practicability in real biological samples. Our research offers a kind of promising peroxidase mimic that may find widespread applications in related fields and provide new insights for fabricating unique catalysts by simultaneously taking advantage of amorphization and other strategies.

EXPERIMENTAL SECTION

Preparation of PtRuTe-HA, PtRuTe-LA, and PtTe Nanomaterials

To synthesize PtRuTe-HA, we mixed 10 mg of $Pt(acac)_2$, 20 mg of $Ru(acac)_3$, 12 mg of $Te(OH)_6$, 3 mg of $Mo(CO)_6$, 25 mg of phloroglucinol, and 200 mg of PVP in 10 mL of DMAC. Before being transferred to a 20 mL Teflon-lined stainless-steel autoclave, the mixture was subjected to ultrasonication for 1 h. The autoclave was then heated from room temperature to 200 °C and maintained at this temperature for 8 h. After being naturally cooled to room temperature, the product was collected by centrifugation and cleaned by a mixture of ethanol and acetone. By reducing the added amount of $Ru(acac)_3$ to 10 mg and 0 mg, PtRuTe-LA and PtTe nanomaterials can be prepared with a similar synthesis procedure as for PtRuTe-HA.

To prepare PtRuTe nanomaterials (PtRuTe-C) with better crystallinity, we first deposited PtRuTe-HA on Ketjen Black-300J carbon via sonicating in ethanol and then collected it by centrifugation. The products were further annealed at 250 °C for 5 h in Ar and 250 °C for 1 h in air.

ASSOCIATED CONTENT

Supporting Information

The Supporting Information is available free of charge at https://pubs.acs.org/doi/10.1021/jacsau.2c00495.

Additional experimental procedures, experimental data such as HRTEM image, characterization data, supporting results, a series of tables, and references (PDF)

AUTHOR INFORMATION

Corresponding Authors

Jing Li − *State Key Laboratory of Electroanalytical Chemistry, Changchun Institute of Applied Chemistry, Chinese Academy of Sciences, Changchun 130022, China;* orcid.org/0000-0002-9828-7569; Email: guosj@pku.edu.cn

Shaojun Guo − *School of Materials Science and Engineering, Peking University, Beijing 100871, China;* orcid.org/0000-0003-4427-6837; Email: lijingce@ciac.ac.cn

Authors

Changshuai Shang − *School of Materials Science and Engineering, Peking University, Beijing 100871, China; State Key Laboratory of Electroanalytical Chemistry, Changchun Institute of Applied Chemistry, Chinese Academy of Sciences, Changchun 130022, China;* orcid.org/0000-0001-7747-6662

Qingqing Wang − *Key Laboratory of Superlight Materials and Surface Technology (Ministry of Education) College of Materials Science and Chemical Engineering, Harbin Engineering University, Harbin 150001, China*

Hao Tan − *School of Materials Science and Engineering, Peking University, Beijing 100871, China*

Shiyu Lu − *School of Materials Science and Engineering, Peking University, Beijing 100871, China*

Shuguang Wang − *School of Materials Science and Engineering, Peking University, Beijing 100871, China*

Qinghua Zhang − *Beijing National Laboratory for Condensed Matter Physics, Institute of Physics, Chinese Academy of Sciences, Beijing 100190, China*

https://doi.org/10.1021/jacsau.2c00495
JACS Au 2022, 2, 2453−2459

Lin Gu − *Beijing National Laboratory for Condensed Matter Physics, Institute of Physics, Chinese Academy of Sciences, Beijing 100190, China;* orcid.org/0000-0002-7504-031X

Erkang Wang − *State Key Laboratory of Electroanalytical Chemistry, Changchun Institute of Applied Chemistry, Chinese Academy of Sciences, Changchun 130022, China;* orcid.org/0000-0001-9843-1834

Complete contact information is available at: https://pubs.acs.org/10.1021/jacsau.2c00495

Notes

The authors declare no competing financial interest.

■ ACKNOWLEDGMENTS

This study was financially supported by National Science Fund for Distinguished Young Scholars (52025133), the National Key R&D Program of China (2019YFA0709202), Tencent Foundation through the XPLORER PRIZE, the Beijing Natural Science Foundation (JQ18005), the Fund of the State Key Laboratory of Solidification Processing in NWPU (SKLSP202004), Youth Innovation Promotion Association (202055), the National Natural Science Foundation of China (22105007), and the China Postdoctoral Science Foundation (2020M670018).

■ REFERENCES

(1) Wu, J.; Wang, X.; Wang, Q.; Lou, Z.; Li, S.; Zhu, Y.; Qin, L.; Wei, H. Nanomaterials with enzyme-like characteristics (nanozymes): next-generation artificial enzymes (II). *Chem. Soc. Rev.* **2019**, *48* (4), 1004−1076.

(2) Wei, H.; Wang, E. Nanomaterials with enzyme-like characteristics (nanozymes): next-generation artificial enzymes. *Chem. Soc. Rev.* **2013**, *42* (14), 6060−6093.

(3) Huang, Y.; Ren, J.; Qu, X. Nanozymes: Classification, Catalytic Mechanisms, Activity Regulation, and Applications. *Chem. Rev.* **2019**, *119* (6), 4357−4412.

(4) Wu, W.; Huang, L.; Wang, E.; Dong, S. Atomic engineering of single-atom nanozymes for enzyme-like catalysis. *Chem. Sci.* **2020**, *11* (36), 9741−9756.

(5) Chen, J.; Ma, Q.; Li, M.; Chao, D.; Huang, L.; Wu, W.; Fang, Y.; Dong, S. Glucose-oxidase like catalytic mechanism of noble metal nanozymes. *Nat. Commun.* **2021**, *12* (1), 3375.

(6) Ji, S.; Jiang, B.; Hao, H.; Chen, Y.; Dong, J.; Mao, Y.; Zhang, Z.; Gao, R.; Chen, W.; Zhang, R.; Liang, Q.; Li, H.; Liu, S.; Wang, Y.; Zhang, Q.; Gu, L.; Duan, D.; Liang, M.; Wang, D.; Yan, X.; Li, Y. Matching the kinetics of natural enzymes with a single-atom iron nanozyme. *Nat. Catal.* **2021**, *4* (5), 407−417.

(7) Gao, L.; Zhuang, J.; Nie, L.; Zhang, J.; Zhang, Y.; Gu, N.; Wang, T.; Feng, J.; Yang, D.; Perrett, S.; Yan, X. Intrinsic peroxidase-like activity of ferromagnetic nanoparticles. *Nat. Nanotechnol.* **2007**, *2* (9), 577−583.

(8) Li, M.; Chen, J.; Wu, W.; Fang, Y.; Dong, S. Oxidase-like MOF-818 Nanozyme with High Specificity for Catalysis of Catechol Oxidation. *J. Am. Chem. Soc.* **2020**, *142* (36), 15569−15574.

(9) Huang, L.; Chen, J.; Gan, L.; Wang, J.; Dong, S. Single-atom nanozymes. *Sci. Adv.* **2019**, *5* (5), No. eaav5490.

(10) Liang, M.; Yan, X. Nanozymes: From New Concepts, Mechanisms, and Standards to Applications. *Acc. Chem. Res.* **2019**, *52* (8), 2190−2200.

(11) Liang, X.; Han, L. White Peroxidase-Mimicking Nanozymes: Colorimetric Pesticide Assay without Interferences of O2 and Color. *Adv. Funct. Mater.* **2020**, *30* (28), 2001933.

(12) Hu, Y.; Gao, X. J.; Zhu, Y.; Muhammad, F.; Tan, S.; Cao, W.; Lin, S.; Jin, Z.; Gao, X.; Wei, H. Nitrogen-Doped Carbon Nanomaterials as Highly Active and Specific Peroxidase Mimics. *Chem. Mater.* **2018**, *30* (18), 6431−6439.

(13) Ge, C.; Wu, R.; Chong, Y.; Fang, G.; Jiang, X.; Pan, Y.; Chen, C.; Yin, J.-J. Synthesis of Pt Hollow Nanodendrites with Enhanced Peroxidase-Like Activity against Bacterial Infections: Implication for Wound Healing. *Adv. Funct. Mater.* **2018**, *28* (28), 1801484.

(14) Xi, Z.; Wei, K.; Wang, Q.; Kim, M. J.; Sun, S.; Fung, V.; Xia, X. Nickel-Platinum Nanoparticles as Peroxidase Mimics with a Record High Catalytic Efficiency. *J. Am. Chem. Soc.* **2021**, *143* (7), 2660−2664.

(15) Wang, Y.; Jia, G.; Cui, X.; Zhao, X.; Zhang, Q.; Gu, L.; Zheng, L.; Li, L. H.; Wu, Q.; Singh, D. J.; Matsumura, D.; Tsuji, T.; Cui, Y.-T.; Zhao, J.; Zheng, W. Coordination Number Regulation of Molybdenum Single-Atom Nanozyme Peroxidase-like Specificity. *Chem.* **2021**, *7* (2), 436−449.

(16) Chen, Y.; Lai, Z.; Zhang, X.; Fan, Z.; He, Q.; Tan, C.; Zhang, H. Phase engineering of nanomaterials. *Nat. Rev. Chem.* **2020**, *4* (5), 243−256.

(17) Wu, G.; Zheng, X.; Cui, P.; Jiang, H.; Wang, X.; Qu, Y.; Chen, W.; Lin, Y.; Li, H.; Han, X.; et al. A general synthesis approach for amorphous noble metal nanosheets. *Nat. Commun.* **2019**, *10* (1), 4855.

(18) Yang, N.; Cheng, H.; Liu, X.; Yun, Q.; Chen, Y.; Li, B.; Chen, B.; Zhang, Z.; Chen, X.; Lu, Q.; Huang, J.; Huang, Y.; Zong, Y.; Yang, Y.; Gu, L.; Zhang, H. Amorphous/Crystalline Hetero-Phase Pd Nanosheets: One-Pot Synthesis and Highly Selective Hydrogenation Reaction. *Adv. Mater.* **2018**, *30* (39), 1803234.

(19) Lv, F.; Zhang, W.; Sun, M.; Lin, F.; Wu, T.; Zhou, P.; Yang, W.; Gao, P.; Huang, B.; Guo, S. Au Clusters on Pd Nanosheets Selectively Switch the Pathway of Ethanol Electrooxidation: Amorphous/Crystalline Interface Matters. *Adv. Energy Mater.* **2021**, *11* (19), 2100187.

(20) Wang, J.; Han, L.; Huang, B.; Shao, Q.; Xin, H. L.; Huang, X. Amorphization activated ruthenium-tellurium nanorods for efficient water splitting. *Nat. Commun.* **2019**, *10* (1), 5692.

(21) Pei, Y.; Zhou, G.; Luan, N.; Zong, B.; Qiao, M.; Tao, F. Synthesis and catalysis of chemically reduced metal-metalloid amorphous alloys. *Chem. Soc. Rev.* **2012**, *41* (24), 8140−8162.

(22) Zhang, X.; Luo, Z.; Yu, P.; Cai, Y.; Du, Y.; Wu, D.; Gao, S.; Tan, C.; Li, Z.; Ren, M.; Osipowicz, T.; Chen, S.; Jiang, Z.; Li, J.; Huang, Y.; Yang, J.; Chen, Y.; Ang, C. Y.; Zhao, Y.; Wang, P.; Song, L.; Wu, X.; Liu, Z.; Borgna, A.; Zhang, H. Lithiation-induced amorphization of Pd3P2S8 for highly efficient hydrogen evolution. *Nat. Catal.* **2018**, *1* (6), 460−468.

(23) Nai, J.; Yin, H.; You, T.; Zheng, L.; Zhang, J.; Wang, P.; Jin, Z.; Tian, Y.; Liu, J.; Tang, Z.; Guo, L. Efficient Electrocatalytic Water Oxidation by Using Amorphous Ni-Co Double Hydroxides Nanocages. *Adv. Energy Mater.* **2015**, *5* (10), 1401880.

(24) Poon, K. C.; Tan, D. C. L.; Vo, T. D. T.; Khezri, B.; Su, H.; Webster, R. D.; Sato, H. Newly Developed Stepwise Electroless Deposition Enables a Remarkably Facile Synthesis of Highly Active and Stable Amorphous Pd Nanoparticle Electrocatalysts for Oxygen Reduction Reaction. *J. Am. Chem. Soc.* **2014**, *136* (14), 5217−5220.

(25) Hashimoto, K. What we have learned from studies on chemical properties of amorphous alloys? *Appl. Surf. Sci.* **2011**, *257* (19), 8141−8150.

(26) Feng, Y.; Huang, B.; Yang, C.; Shao, Q.; Huang, X. Platinum Porous Nanosheets with High Surface Distortion and Pt Utilization for Enhanced Oxygen Reduction Catalysis. *Adv. Funct. Mater.* **2019**, *29* (45), 1904429.

(27) Shang, C.; Guo, Y.; Wang, E. Ultrathin nanodendrite surrounded PtRuNi nanoframes as efficient catalysts for methanol electrooxidation. *J. Mater. Chem. A* **2019**, *7* (6), 2547−2552.

(28) Zhang, J.; Yin, R.; Shao, Q.; Zhu, T.; Huang, X. Oxygen Vacancies in Amorphous InOx Nanoribbons Enhance CO2 Adsorption and Activation for CO2 Electroreduction. *Angew. Chem., Int. Ed.* **2019**, *58* (17), 5609−5613.

(29) Yu, B.; Wang, W.; Sun, W.; Jiang, C.; Lu, L. Defect Engineering Enables Synergistic Action of Enzyme-Mimicking Active Centers for

High-Efficiency Tumor Therapy. *J. Am. Chem. Soc.* **2021**, *143* (23), 8855−8865.
(30) Josephy, P. D.; Eling, T.; Mason, R. P. The horseradish peroxidase-catalyzed oxidation of 3,5,3′,5′-tetramethylbenzidine. Free radical and charge-transfer complex intermediates. *J. Biol. Chem.* **1982**, *257* (7), 3669−3675.
(31) Yan, H.; Chen, Y.; Jiao, L.; Gu, W.; Zhu, C. Amorphous RuTe2 nanorods as efficient peroxidase mimics for colorimetric immunoassay. *Sens. Actuators, B* **2021**, *341*, 130007.
(32) Song, Y.; Qu, K.; Zhao, C.; Ren, J.; Qu, X. Graphene Oxide: Intrinsic Peroxidase Catalytic Activity and Its Application to Glucose Detection. *Adv. Mater.* **2010**, *22* (19), 2206−2210.
(33) Wei, Z.; Xi, Z.; Vlasov, S.; Ayala, J.; Xia, X. Nanocrystals of platinum-group metals as peroxidase mimics for in vitro diagnostics. *Chem. Commun.* **2020**, *56* (95), 14962−14975.
(34) Shang, C.; Guo, Y.; Wang, E. Facile fabrication of PdRuPt nanowire networks with tunable compositions as efficient methanol electrooxidation catalysts. *Nano Res.* **2018**, *11* (8), 4348−4355.
(35) Tong, D.-G.; Chu, W.; Luo, Y.-Y.; Ji, X.-Y.; He, Y. Effect of crystallinity on the catalytic performance of amorphous Co-B particles prepared from cobalt nitrate and potassium borohydride in the cinnamaldehyde hydrogenation. *J. Mol. Catal. A: Chem.* **2007**, *265* (1), 195−204.
(36) Xi, Z.; Cheng, X.; Gao, Z.; Wang, M.; Cai, T.; Muzzio, M.; Davidson, E.; Chen, O.; Jung, Y.; Sun, S.; Xu, Y.; Xia, X. Strain Effect in Palladium Nanostructures as Nanozymes. *Nano Lett.* **2020**, *20* (1), 272−277.
(37) Li, J.; Liu, W.; Wu, X.; Gao, X. Mechanism of pH-switchable peroxidase and catalase-like activities of gold, silver, platinum and palladium. *Biomaterials* **2015**, *48*, 37−44.
(38) Kim, M. S.; Cho, S.; Joo, S. H.; Lee, J.; Kwak, S. K.; Kim, M. I.; Lee, J. N- and B-Codoped Graphene: A Strong Candidate To Replace Natural Peroxidase in Sensitive and Selective Bioassays. *ACS Nano* **2019**, *13* (4), 4312−4321.
(39) Kim, M. S.; Lee, J.; Kim, H. S.; Cho, A.; Shim, K. H.; Le, T. N.; An, S. S. A.; Han, J. W.; Kim, M. I.; Lee, J. Heme Cofactor-Resembling Fe-N Single Site Embedded Graphene as Nanozymes to Selectively Detect H2O2 with High Sensitivity. *Adv. Funct. Mater.* **2020**, *30* (1), 1905410.
(40) Wei, H.; Wang, E. Fe3O4Magnetic Nanoparticles as Peroxidase Mimetics and Their Applications in H2O2 and Glucose Detection. *Anal. Chem.* **2008**, *80* (6), 2250−2254.
(41) Wang, Q.; Zhang, X.; Huang, L.; Zhang, Z.; Dong, S. GOx@ZIF-8(NiPd) Nanoflower: An Artificial Enzyme System for Tandem Catalysis. *Angew. Chem., Int. Ed.* **2017**, *56* (50), 16082−16085.
(42) Ma, C.-B.; Zhang, Y.; Liu, Q.; Du, Y.; Wang, E. Enhanced Stability of Enzyme Immobilized in Rationally Designed Amphiphilic Aerogel and Its Application for Sensitive Glucose Detection. *Anal. Chem.* **2020**, *92* (7), 5319−5328.

https://doi.org/10.1021/jacsau.2c00495
JACS Au 2022, 2, 2453−2459